Correlation functions and electronic noise in doped semiconductors

Tilmann Kuhn,* Lino Reggiani, and Luca Varani
Dipartimento di Fisica e Centro Interuniversitario di Struttura della Materia, Università degli Studi di Modena, via Campi 213/A, I-41100 Modena, Italy
(Received 25 May 1990)

We present an original Monte Carlo study of correlation functions for the general case of a doped semiconductor under the influence of an electric field of arbitrary strength. Number, velocity, and energy of the carriers are taken as relevant variables. These lead to a set of 25 correlation functions that, for the case of a cubic semiconductor and an electric field in the ⟨100⟩ direction as investigated in this paper, reduce to 11 nonvanishing functions. By using an analytical model based on coupled Langevin equations together with the results of the Monte Carlo simulations, we have quantitatively analyzed the different coupling processes as functions of the electric field. The simulations are performed for lightly doped *p*-type Si at 77 K. We demonstrate that even at equilibrium the coupling between energy relaxation and generation-recombination processes can lead to a strongly nonexponential decay of the corresponding correlation functions. At higher fields, we find the interesting result of a transition from two real relaxation rates for energy and longitudinal velocity to a pair of complex-conjugate values, which indicates some kind of ordering in the system driven by the electric field. At the highest fields, this ordering disappears and the rates again become real. The theory so developed is shown to provide a rigorous scheme for a microscopic interpretation of noise-spectroscopy measurement.

I. INTRODUCTION

The use of correlation functions has been proven to be a fundamental tool for the description of a statistical ensemble of charge carriers, both at equilibrium[1-3] and for nonequilibrium conditions.[4-7] Indeed, phenomenological coefficients describing many transport processes and time-dependent phenomena in general can be written as time integrals of these functions which, in turn, provide also valuable information on the characteristic relaxation processes of the system. The experimental counterparts of these functions have been traditionally the electro-optical spectroscopy measurements.[8,9] However, in recent years measurements of the current spectral density in the region of high frequencies (which avoids $1/f$ noise) have been performed by several international groups, e.g., in Gainsville, Minneapolis, Montpellier, Utrecht, and Vilnius.[10] This so-called noise spectroscopy is offering an appealing opportunity to check the physical plausibility of the correlation functions. Because of its fundamental interest and technological importance, the possibility to provide a microscopic interpretation of noise spectra has been considered a worthwhile subject to be pursued.

The aim of this paper is to present a theoretical study of the correlation functions for the case of a doped semiconductor under the influence of an electric field of arbitrary strength. To this end, by generalizing the results given in a previous paper,[7] we consider as the relevant set of variables the concentration of carriers in the conducting band, the three components of their velocity, and their kinetic energy. This, in turn, leads in general to a set of 25 correlation functions whose properties are studied for the case of a cubic semiconductor. Then, by using a Monte Carlo (MC) simulation together with a theoretical approach which provides smooth analytical expressions for the correlation functions, their time dependence is analyzed at increasing electric fields, when hot-carrier conditions set in. Calculations are applied to the case of *p*-type Si at 77 K for an acceptor concentration $N_A = 3\times10^{15}$ cm^{-3} where a set of experiments from Vaissiere and co-workers is available.[11,12] In this case, at equilibrium the fraction of free carriers is significantly less than unity because of impurity freeze out and so, under far from equilibrium conditions, we are in the presence of a field assisted ionization. Finally, particular attention will be paid to the correlation functions which contribute directly to the current-current fluctuations correlator, which forms the basis for the interpretation of noise measurements.

The paper is organized as follows: Sec. II presents the theory for a rigorous definition of different correlation functions within a particle approach appropriate to the MC method. In Sec. III simulation, as applied to the case of *p*-type Si is described. A theory which provides analytical expressions for the correlation functions is given in Sec. IV. Section V reports the results for the current spectral density and the main features in terms of the different relaxation times which characterize the carrier ensemble are discussed which are appropriate for the analysis of experimental data. The main conclusions are drawn in Sec. V. Two appendixes, which complement the theory, are finally added.

II. THEORY

We consider a uniform semiconductor sample of cross-sectional area A and length L in which charge transport occurs through a two-level system: the con-

ducting band and the impurity centers which supply the carriers. Let N_I be the total number of available carriers, which equals the number of impurity centers, and $N(t)$ the number of free carriers in the conducting band. As relevant variables we take the counterpart of the macrovariables which define a heated and displaced Maxwellian distribution, i.e., the average number of particles, the three components of their average velocity, and their average kinetic energy. These quantities more generally represent the first three moments of the actual distribution. Accordingly, the fraction of free carriers $u(t)$ is given by

$$u(t)=\frac{1}{N_I}\sum_{i=1}^{N_I}u_i(t)=\frac{N(t)}{N_I}\ , \tag{1}$$

where $u_i(t)$ is the random telegraph signal:

$$u_i(t)=\begin{cases}1 & \text{if carrier is free}\\ 0 & \text{if carrier is trapped.}\end{cases} \tag{2}$$

The average velocity $\mathbf{v}(t)$, and the average (kinetic) energy per carrier $\varepsilon(t)$ can be given the two following equivalent definitions: (i) with respect to the number of carriers in the band:

$$\mathbf{v}(t)=\frac{1}{N(t)}\sum_{i=1}^{N(t)}\mathbf{v}_i(t)\ , \tag{3}$$

$$\varepsilon(t)=\frac{1}{N(t)}\sum_{i=1}^{N(t)}\varepsilon_i(t)\ , \tag{4}$$

where subscripts i refer to the ith carrier; (ii) with respect to the total number of carriers:

$$\mathbf{v}(t)=\frac{\mathbf{v}^r(t)}{u(t)}=\frac{1}{u(t)N_I}\sum_{i=1}^{N_I}\mathbf{v}_i^r(t)\ , \tag{5}$$

$$\varepsilon(t)=\frac{\varepsilon^r(t)}{u(t)}=\frac{1}{u(t)N_I}\sum_{i=1}^{N_I}\varepsilon_i^r(t)\ , \tag{6}$$

where $\mathbf{v}_i^r(t)$ is the reduced velocity of the single carrier defined as

$$\mathbf{v}_i^r(t)=\begin{cases}\mathbf{v}_i(t) & \text{if carrier is free}\\ 0 & \text{if carrier is trapped}\end{cases} \tag{7}$$

and $\varepsilon_i^r(t)$ is the reduced energy of the single carrier defined as

$$\varepsilon_i^r(t)=\begin{cases}\varepsilon_i(t) & \text{if carrier is free}\\ 0 & \text{if carrier is trapped.}\end{cases} \tag{8}$$

The definitions in Eqs. (1)–(8) enable one to write the total current induced in the external circuit $I(t)$ and the total kinetic energy $\varepsilon_{\rm tot}(t)$ in the two equivalent forms (see Appendix A of Ref. 11 for a discussion concerning the definition of the total current):

$$I(t)=\frac{e}{L}N(t)v_l(t)=\frac{e}{L}N_Iv_l^r(t)\ , \tag{9}$$

$$\varepsilon_{\rm tot}(t)=N(t)\varepsilon(t)=N_I\varepsilon^r(t)\ , \tag{10}$$

$v_l(t)$ and $v_l^r(t)$ being the component of the average velocity and reduced velocity along the direction of current flow. Thus, the use of the reduced quantities enables one to describe the time dependence of the total current and the total kinetic energy in terms of a single time dependent variable, respectively. Furthermore, within case (ii) the summation to obtain average quantities is always extended over all carriers. This property, as will be discussed later, allows their calculation within a single particle approximation.

The temporal behavior of fluctuations around a stationary state is described by single-time correlation functions of the type $\overline{\delta A(0)\delta B(t)}$ with $\delta B(t)=B(t)-\bar{B}$, the bar indicating time averages, where A and B stay for any of the five relevant variables considered above. (We assume ergodicity, so that time averages are equivalent to ensemble averages.) Since the electric field defines a preferential direction in the system, with respect to this direction we take for the average velocity a longitudinal, v_l, and two transverse, v_{t1} and v_{t2}, components, respectively. Therefore, a set of 25 correlation functions is required to describe the present physical system. These can be grouped into four scalar, four vector, and one tensorlike quantities, respectively. In general, all 25 correlation functions are different. However, in a cubic crystal with an electric field $\mathbf{E}$ parallel to the $\langle 100\rangle$ crystallographic direction, for symmetry reasons only 11 differ from zero, the two autocorrelation functions of the transverse velocities being identical. Indeed, since the electric field is in a high-symmetry direction, all vectorlike correlation functions must also be in this direction. Furthermore, the tensorlike function must be diagonal with two identical components. As a consequence, all cross-correlation functions with transverse velocities vanish.

By using the shorthand notation $\Phi_{AB}=\overline{\delta A(0)\delta B(t)}$, $\Phi^r_{AB}=\overline{\delta A^r(0)\delta B^r(t)}$, the 11 correlation functions are related to the corresponding reduced correlation functions by the following relationships (see Appendix A):

$$\Phi_{uu}=\Phi^r_{uu}\ , \tag{11}$$

$$\Phi_{v_lv_l}=\frac{1}{\bar{u}^2}[\Phi^r_{v_lv_l}+\bar{v}_l^2\Phi^r_{uu}-\bar{v}_l(\Phi^r_{v_lu}+\Phi^r_{uv_l})]\ , \tag{12}$$

$$\Phi_{v_{t1}v_{t1}}=\Phi_{v_{t2}v_{t2}}=\frac{1}{\bar{u}^2}\Phi^r_{v_{t1}v_{t1}}\ , \tag{13}$$

$$\Phi_{\varepsilon\varepsilon}=\frac{1}{\bar{u}^2}[\Phi^r_{\varepsilon\varepsilon}+\bar{\varepsilon}^2\Phi^r_{uu}-\bar{\varepsilon}(\Phi^r_{u\varepsilon}+\Phi^r_{\varepsilon u})]\ , \tag{14}$$

$$\Phi_{uv_l}=\frac{1}{\bar{u}}(\Phi^r_{uv_l}-\bar{v}_l\Phi^r_{uu})\ , \tag{15}$$

$$\Phi_{v_lu}=\frac{1}{\bar{u}}(\Phi^r_{v_lu}-\bar{v}_l\Phi^r_{uu})\ , \tag{16}$$

$$\Phi_{u\varepsilon}=\frac{1}{\bar{u}}(\Phi^r_{u\varepsilon}-\bar{\varepsilon}\Phi^r_{uu})\ , \tag{17}$$

$$\Phi_{\varepsilon u}=\frac{1}{\bar{u}}(\Phi^r_{\varepsilon u}-\bar{\varepsilon}\Phi^r_{uu})\ , \tag{18}$$

$$\Phi_{\varepsilon v_l}=\frac{1}{\bar{u}^2}(\Phi^r_{\varepsilon v_l}+\bar{v}_l\bar{\varepsilon}\Phi^r_{uu}-\bar{v}_l\Phi^r_{\varepsilon u}-\bar{\varepsilon}\Phi^r_{uv_l})\ , \tag{19}$$

$$\Phi_{v_l\varepsilon}=\frac{1}{\bar{u}^2}(\Phi^r_{v_l\varepsilon}+\bar{v}_l\bar{\varepsilon}\Phi^r_{uu}-\bar{v}_l\Phi^r_{u\varepsilon}-\bar{\varepsilon}\Phi^r_{v_lu})\ . \tag{20}$$

III. MONTE CARLO SIMULATION

Calculations are performed for the case of p-type Si (boron doped) with an acceptor concentration $N_A = 3\times10^{15}$ cm^{-3}, where recent noise experiments from Vaissiere and co-workers[11,12] are available. As generation-recombination (GR) mechanism we take the capture assisted by long-wavelength acoustic phonons, which in the present case is expected to be the most relevant process. The details of the microscopic model are those given in Ref. 13, and the parameters entering the simulation are summarized in Table I. To simplify the calculations and make the central-processing-unit (CPU) time accessible, we consider the case of noninteracting particles. (Here, particle-particle interaction means not only a direct scattering between two carriers, but also a correlation introduced by the occupancy factor of the impurity levels. Thus, for a single particle simulation only a linear recombination can be treated.) In this case we can take advantage of the representation in terms of the reduced velocity and reduced energy seen above and calculate the different correlation functions from a one-particle approach. For this purpose, we make use of the following properties (see Appendix B):

$$\Phi^r_{AB} = \frac{1}{N_I}\Phi^r_{A_iB_i} , \tag{21}$$

where subscripts i refer to a single carrier.

The different reduced correlation functions are evaluated in the standard way, as for the case of the autocorrelation function of velocity fluctuations in the absence of GR processes.[14] To this end we record the instantaneous values of $u_i(t)$, $\mathbf{v}^r_i(t)$, and $\varepsilon^r_i(t)$ on time steps sufficiently small to reproduce the characteristic features of the correlation functions. Typical time steps are in the range from 5×10^{-15} s for the correlation functions of the velocity at very high fields up to 10^{-11} s for the correlation function of particle number. The correlation functions are then calculated as time averages of the products of these variables with a given delay time. In order to obtain sufficiently smooth correlation functions, the total simulation time should be of the order of 100 ns. The average fraction of ionized carriers is consistently determined from the ratio between the total time spent in the valence band and the total time of the simulation. Each simulation requires between 2 and 10 h CPU time of a Digital Equipment Corporation VAX 6310. The reason for these long times is the large difference in the time scales involved in the problem: scatterings occur typically on a time scale below 1 ps while the time scale for GR processes is of the order of 100 ps to 1 ns.

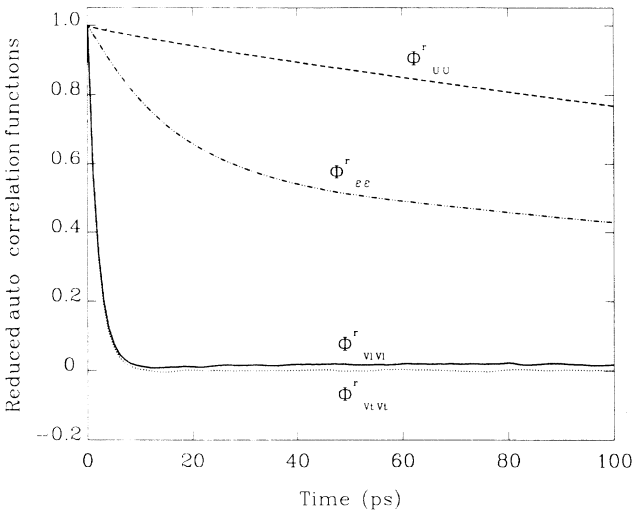

FIG. 1. Reduced autocorrelation functions normalized to their initial values in p-type Si at 77 K with $N_A = 3\times10^{15}$ cm^{-3} at an electric field of 250 V/cm as a function of time obtained as direct output from the MC simulation. Continuous, dotted, dashed, and dash-dotted lines refer, respectively, to $\Phi^r_{v_lv_l}(t)$, $\Phi^r_{v_tv_t}(t)$, $\Phi^r_{uu}(t)$, and $\Phi^r_{\varepsilon\varepsilon}(t)$.

Finally, because of the linear recombination here considered, we notice the following zero time properties of some correlation functions:

$$\Phi_{uu}(0) = \bar{u}(1-\bar{u}) , \tag{22}$$

$$\Phi_{uv_l}(0) = \Phi_{u\varepsilon}(0) = 0 . \tag{23}$$

The results of the simulation for a low-field case of 250 V/cm are reported in Figs. 1–4. Figures 1 and 2 refer to

TABLE I. Parameters for p-type Si used in calculations. The effective mass takes into account nonparabolicity and therefore it varies as a function of carrier mean energy between the given values as reported in Ref. 15.

Parameter	Value
effective mass	$m_h = (0.53\text{–}1.26)m_0$
crystal density	$\rho_0 = 2.32$ g cm^{-3}
sound velocity	$s = 6.53\times10^5$ cm s^{-1}
optical-phonon temperature	$\theta_{op} = 735$ K
relative static dielectric constant	$\epsilon_0 = 11.7$
acoustic deformation potential	$E_1^0 = 5$ eV
optical deformation potential	$D_tK = 6\times10^8$ eV cm^{-1}
equilibrium volume recombination rate	$\rho_{eq} = 4.2\times10^{-6}$ cm^3 s^{-1}
equilibrium generation rate	$\gamma_{eq} = 2.9\times10^9$ s^{-1}
energy of the acceptor level	$\varepsilon_a = 45$ meV
cross section for impact ionization	$\sigma_g = 5.02\times10^{-14}$ cm^2

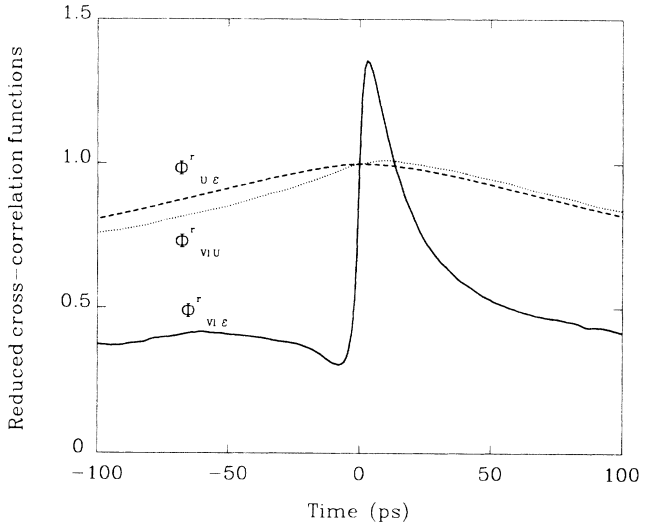

FIG. 2. Reduced cross-correlation functions normalized to their initial values in p-type Si at 77 K with $N_A = 3\times10^{15}$ cm^{-3} at an electric field of 250 V/cm as a function of time obtained as direct output from the MC simulation. Continuous, dotted, and dashed lines refer, respectively, to $\Phi^r_{v_l\varepsilon}(t)$, $\Phi^r_{v_l u}(t)$, and $\Phi^r_{u\varepsilon}(t)$.

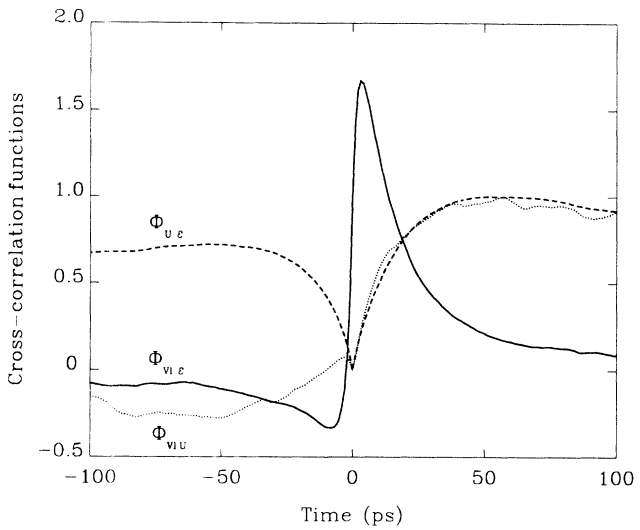

FIG. 4. Cross-correlation functions in p-type Si at 77 K with $N_A = 3\times10^{15}$ cm^{-3} at an electric field of 250 V/cm as a function of time obtained from the MC simulation using Eqs. (15)–(20). Continuous, dotted, and dashed lines refer, respectively, to $\Phi_{v_l\varepsilon}(t)$, $\Phi_{v_l u}(t)$, and $\Phi_{u\varepsilon}(t)$. The function $\Phi_{v_l\varepsilon}(t)$ is normalized to its initial value; other functions, having a zero initial value, are normalized to their maximum.

the reduced correlation functions, which are the direct output of the simulation. Their values are normalized to the initial values at zero time. Figures 3 and 4 refer to the corresponding correlation functions obtained using Eqs. (11)–(20). For the purpose of clarity, the diagonal and off-diagonal terms are displayed separately. Furthermore, the latter ones are drawn on a symmetric time axis using the property $\overline{\delta A(0)\delta B(t)} = \overline{\delta A(-t)\delta B(0)}$ so that each curve corresponds to a couple of terms. Again normalized values are given, the diagonal terms and the off-diagonal velocity-energy correlation function being normalized to their initial values, while the other off-

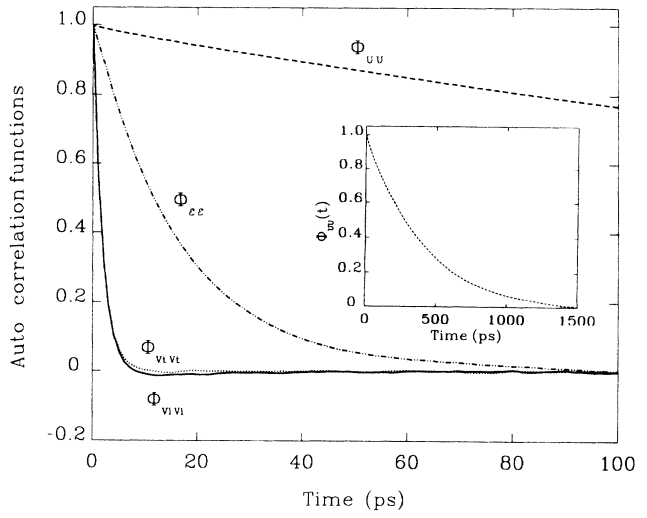

FIG. 3. Autocorrelation functions normalized to their initial values in p-type Si at 77 K with $N_A = 3\times10^{15}$ cm^{-3} at an electric field of 250 V/cm as a function of time obtained from the MC simulation using Eqs. (11)–(14). Continuous, dotted, dashed, and dash-dotted lines refer, respectively, to $\Phi_{v_l v_l}(t)$, $\Phi_{v_t v_t}(t)$, $\Phi_{uu}(t)$, and $\Phi_{\varepsilon\varepsilon}(t)$. The inset shows the long-time decay of $\Phi_{uu}(t)$.

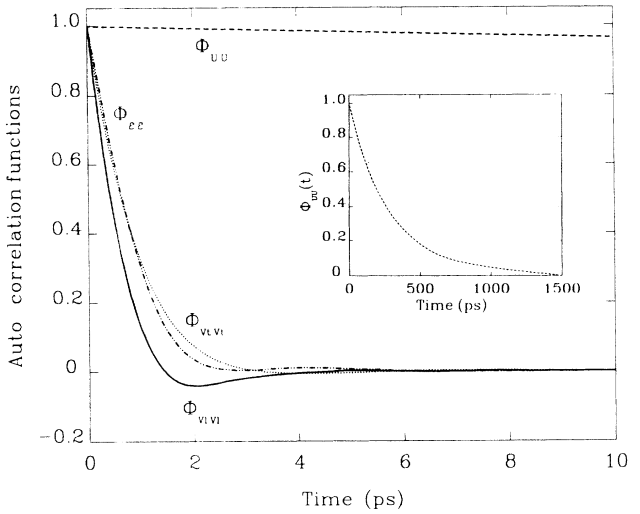

FIG. 5. Autocorrelation functions normalized to their initial values in p-type Si at 77 K with $N_A = 3\times10^{15}$ cm^{-3} at an electric field of 2500 V/cm as a function of time obtained from the MC simulation using Eqs. (11)–(14). Continuous, dotted, dashed, and dash-dotted lines refer, respectively, to $\Phi_{v_l v_l}(t)$, $\Phi_{v_t v_t}(t)$, $\Phi_{uu}(t)$, and $\Phi_{\varepsilon\varepsilon}(t)$. The inset shows the long-time decay of $\Phi_{uu}(t)$.

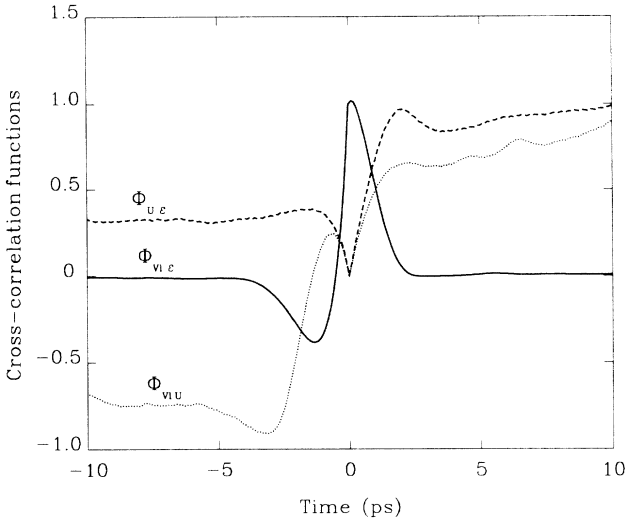

FIG. 6. Cross-correlation functions in p-type Si at 77 K with $N_A = 3\times10^{15}$ cm^{-3} at an electric field of 2500 V/cm as a function of time obtained from the MC simulation using Eqs. (15)–(20). Continuous, dotted, and dashed lines refer, respectively, to $\Phi_{v_l\varepsilon}(t)$, $\Phi_{v_l u}(t)$, and $\Phi_{u\varepsilon}(t)$. The function $\Phi_{v_l\varepsilon}(t)$ is normalized to its initial value; other functions, having a zero initial value, are normalized to their maximum.

diagonal terms, having a zero initial value, are normalized to their maximum value, respectively.

Figure 1 and 2 are appropriate to evidence the time resolution of the numerical calculations, while Figs 3 and 4 enable a physical interpretation to be carried out in terms of four relaxation times. These can be easily identified by the nearly exponential decay of the diagonal terms in Fig. 3 as the velocity relaxation times, related to the longitudinal and transverse velocity fluctuations; the energy relaxation time, related to the energy fluctuations; the lifetime, related to the particle-state fluctuations. For the off-diagonal terms of Fig. 4, it emerges that the different relaxation times are mixed together, each of them playing a role in a restricted time interval.

Figures 5 and 6 show the correlation functions for a higher field of 2500 V/cm. Here, because of the far from equilibrium conditions, even the diagonal correlation functions (see Fig. 5) exhibit structures which strongly deviate from a simple exponential behavior. Table II reports the average values of the relevant variables and the initial and maximum values of the correlation functions shown in Figs. 3–6. To help the physical interpretation, we now combine the results of the MC simulation with a theoretical model which provides analytical expressions for the correlation functions.

TABLE II. Average values of the relevant variables, initial and maximum values of the single particle correlation functions at electric fields of 250 and 2500 V/cm. Calculations refer to the case of p-type Si at 77 K with $N_A = 3\times10^{15}$ cm^{-3}.

Variable	Units	Value $E=250$ V cm^{-1}	Value $E=2500$ V cm^{-1}
$\bar{u}$		0.50	0.70
$\overline{v_l}$	10^6 cm s^{-1}	1.2	4.4
$\bar{\varepsilon}$	meV	17	31
$\Phi_{uu}(0)$		0.25	0.21
$\Phi_{v_l v_l}(0)$	10^{13} cm^2 s^{-2}	7.0	8.8
$\Phi_{v_t v_t}(0)$	10^{13} cm^2 s^{-2}	3.1	3.8
$\Phi_{\varepsilon\varepsilon}(0)$	(meV)^2	310	570
$\Phi_{\varepsilon v_l}(0)$	10^8 meV cm s^{-1}	0.24	1.0
$\max[\Phi_{uv_l}(t)]$	10^3 cm s^{-1}	46.0	7.0
$\max[\Phi_{u\varepsilon}(t)]$	meV	0.49	0.046

IV. ANALYTICAL RESULTS

In the preceding section we have seen that the shapes of the correlation functions (in particular, those of the cross-correlation functions) may be very complicated involving various time scales. In order to obtain a physical interpretation of the MC results we now analyze the correlation functions within the framework of the analytical model of Ref. 7. There, based on a quantum-mechanical derivation of generalized Langevin equations within a projection operator formalism, it has been shown that under suitable approximations (i.e., separation of the time scales between the "relevant" and the "irrelevant" variables and neglect of memory effects) a closed system of equations of motion for the correlation functions of a complete set of relevant variables $P_m, m=1,\ldots,M$ can be obtained in the form

$$\frac{d}{dt}\Phi_{ij}(t) = -\sum_{k=1}^{M}\alpha_{jk}\Phi_{ik}(t)\ , \tag{24}$$

where

$$\Phi_{ij}(t) = \overline{\delta P_i(0)\delta P_j(t)}\ . \tag{25}$$

The important property of Eq. (24) is the fact that the matrix α does not depend on the index i of the first variable. This permits a unique determination of the elements α_{ij} from the knowledge of the initial conditions $\Phi_{ij}(0)$ and $d\Phi_{ij}(0)/dt$. The elements are given by the standard formula:

$$\alpha_{ij} = \frac{D_{ij}}{D}\ , \tag{26}$$

where $D = \det\{\Phi_{kl}(0)\}$ and D_{ij} is the determinant obtained from D, if in column j the values $\Phi_{kj}(0)$ are replaced by $-d\Phi_{ki}(0)/dt$. The general solution of Eq. (24) can be written as

$$\Phi_{ij}(t) = \sum_{\nu=1}^{M}\Phi_{ij}^{(\nu)}(t) = \sum_{\nu=1}^{M} c_i^{(\nu)}\psi_j^{(\nu)}e^{-\lambda^{(\nu)}t} = \sum_{\nu=1}^{M} d_{ij}^{(\nu)}e^{-\lambda^{(\nu)}t}\ , \tag{27}$$

where $\lambda^{(\nu)}$ is the νth eigenvalue of α, $\psi_j^{(\nu)}$ the jth component of the corresponding eigenvector, and $c_i^{(\nu)}$ the expansion coefficient given by the scalar product

$$c_i^{(\nu)}=\sum_{k=1}^{M}\Phi_{ik}(0)\tilde{\psi}_k^{(\nu)} . \tag{28}$$

$\tilde{\psi}_k^{(\nu)}$ is the eigenvector of the transposed matrix α^T corresponding to the eigenvalue $\lambda^{(\nu)}$ and we have assumed that the eigenvectors are normalized, i.e.,

$$\sum_{k=1}^{M}\psi_k^{(\mu)}\tilde{\psi}_k^{(\nu)}=\delta_{\mu\nu} . \tag{29}$$

Since the matrix α in general is not symmetric, the eigenvalues may not only be real, but there can also exist pairs of complex-conjugate values. Because the correlation functions must be real, in this case also the eigenvectors and expansion coefficients must be complex conjugate.

Within the above scheme we are now able to analyze the various correlation functions. The system is described by M eigenvalues $\lambda^{(\nu)}$. If the eigenvalues are real, each value λ can be interpreted as a relaxation rate. On the other hand, each pair of complex-conjugate eigenvalues defines a relaxation rate $\mathrm{Re}(\lambda)$ and an angular frequency $\mathrm{Im}(\lambda)$. The correlation function then has a damped oscillatory contribution

$$\Phi_{ij}^{(\nu)}(t)=2|d^{(\nu)}|e^{-\mathrm{Re}(\lambda^{(\nu)})t}\cos[\mathrm{Im}(\lambda^{(\nu)})t+\chi] , \tag{30}$$

where the phase χ is given by the phase of the corresponding expansion coefficient

$$\chi=\arctan\left[\frac{\mathrm{Im}(d^{(\nu)})}{\mathrm{Re}(d^{(\nu)})}\right] . \tag{31}$$

In general, a correlation function $\Phi_{ij}(t)$ contains an evolution on the time scale of each of these rates and frequencies, their contributions being given by the expansion coefficients $d_{ij}^{(\nu)}$. If in an autocorrelation function $\Phi_{ii}(t)$ one coefficient $d_{ii}^{(\nu)}$ corresponding to a real eigenvalue $\lambda^{(\nu)}$ is dominant with respect to all others, then $\lambda^{(\nu)}$ can be identified as the relaxation rate of the variable P_i. In general, however, due to the coupling between the different variables a rigorous definition of a relaxation rate for each variable is not possible.

In the present work we take as relevant variables the five quantities introduced in Sec. II. As already discussed, for symmetry reasons the transverse velocities do not couple to the other three variables. Thus the matrix α is diagonal with respect to these quantities, the diagonal elements being identical and defining the relaxation rate of the transverse velocity. Effectively, we have to consider only a 3×3 matrix for the variables u, v_l, and ε. Although in Ref. 7 the general formula for the matrix α is derived using a projection operator into the relevant subspace, for any real band-structure and interaction processes it is impossible to be solved analytically. But as has been shown above, α is totally determined by the initial values and derivatives of the correlation functions.

Thus, using the initial values $\Phi_{ij}(0)$ and $d\Phi_{ij}(0)/dt$ from the MC simulation as input we have calculated the matrix α, its eigenvalues, and eigenvectors as well as the expansion of $\Phi_{ij}(t)$ into the sum of the exponential functions in Eq. (27). Figure 7 shows the diagonal correlation function as obtained from the analytical calculations for the case $E=250$ V/cm. It turns out that the agreement between the analytic and the MC results is very good for the case of the three velocity autocorrelation functions (see Fig. 3). The autocorrelation functions of energy and particle state obtained from the MC calculation, however, decay more slowly than their analytical counterparts. The reason is the strong microscopic coupling between scattering and GR processes at low carrier energies, as already discussed in detail in a previous paper.[13] This coupling induces some kind of memory effect leading to a nonexponential decay of the correlation functions which, of course, cannot be explained by the mesoscopic analytical model of Eq. (24). Figure 8 shows the off-diagonal correlation functions whose shapes are in good agreement with MC results. This means that the expansion coefficients $d_{ij}^{(\nu)}$ are the correct ones, even if the long-time behavior of the exponential functions is wrong. In fact, if we replace only the two eigenvalues of the energy and particle state autocorrelation functions by the values obtained from the long-time decay of these functions, we get a satisfactory agreement for all 11 correlation functions.

At increasing electric field strength, due to the onset of hot-carrier conditions, the importance of this microscopic coupling at low energies decreases. This improves the agreement between MC and analytical results, and above about 500 V/cm all autocorrelation functions are well

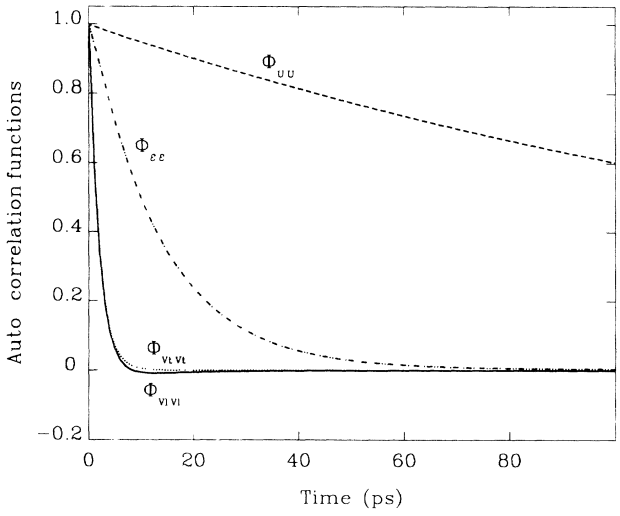

FIG. 7. Autocorrelation functions normalized to their initial values in p-type Si at 77 K with $N_A=3\times10^{15}$ cm^{-3} at an electric field of 250 V/cm as a function of time obtained from the expansion into eigenvectors of the matrix α. Continuous, dotted, dashed, and dash-dotted lines refer, respectively, to $\Phi_{v_l v_l}(t)$, $\Phi_{v_t v_t}(t)$, $\Phi_{uu}(t)$, and $\Phi_{\varepsilon\varepsilon}(t)$.

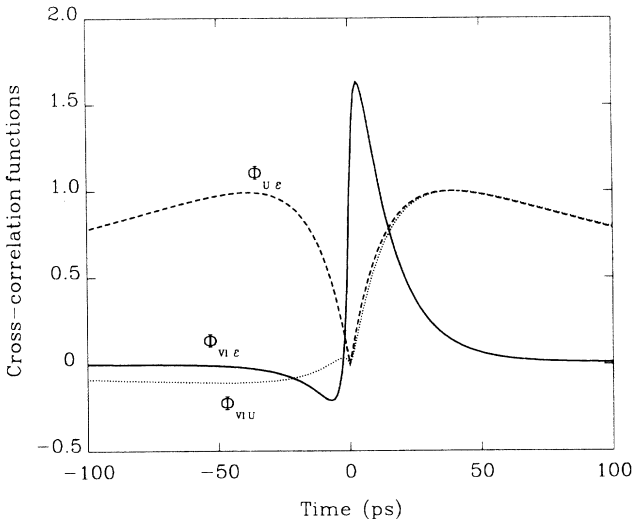

FIG. 8. Cross-correlation functions in p-type Si at 77 K with $N_A = 3\times10^{15}$ cm^{-3} at an electric field of 250 V/cm as a function of time obtained from the expansion into eigenvectors of the matrix α. Continuous, dotted, and dashed lines refer, respectively, to $\Phi_{v_l\varepsilon}(t)$, $\Phi_{v_l u}(t)$, and $\Phi_{u\varepsilon}(t)$. The function $\Phi_{v_l\varepsilon}(t)$ is normalized to its initial value; other functions, having a zero initial value, are normalized to their maximum.

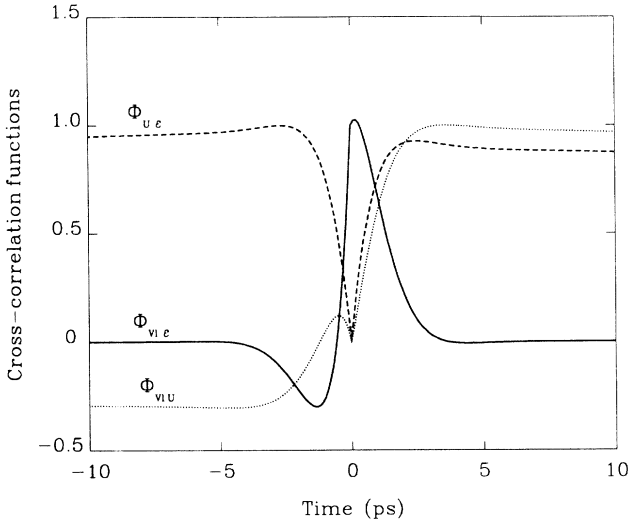

FIG. 10. Cross-correlation functions in p-type Si at 77 K with $N_A = 3\times10^{15}$ cm^{-3} at an electric field of 2500 V/cm as a function of time obtained from the expansion into eigenvectors of the matrix α. Continuous, dotted, and dashed lines refer, respectively, to $\Phi_{v_l\varepsilon}(t)$, $\Phi_{v_l u}(t)$, and $\Phi_{u\varepsilon}(t)$. The function $\Phi_{v_l\varepsilon}(t)$ is normalized to its initial value; other functions, having a zero initial value, are normalized to their maximum.

reproduced. A typical example is shown in Figs. 9 and 10 which report the diagonal and off-diagonal terms at an intermediate field of 2500 V/cm. Finally, at the highest field strengths starting at about 5000 V/cm the agreement, especially for the case of the velocity and energy autocorrelation functions, becomes slightly worse. Probably, in this strong far from equilibrium regime the chosen variables do not constitute anymore a complete set of relevant variables. In fact, preliminary studies suggest that correlation functions involving higher moments of velocity and energy now do not decay much faster than those of the chosen low-order moments. Thus the assumed possibility of decomposing the time scales into slow and fast components is no longer valid. However, even in this case the qualitative behavior of all 11 correlation functions is well reproduced by the analytical solutions.

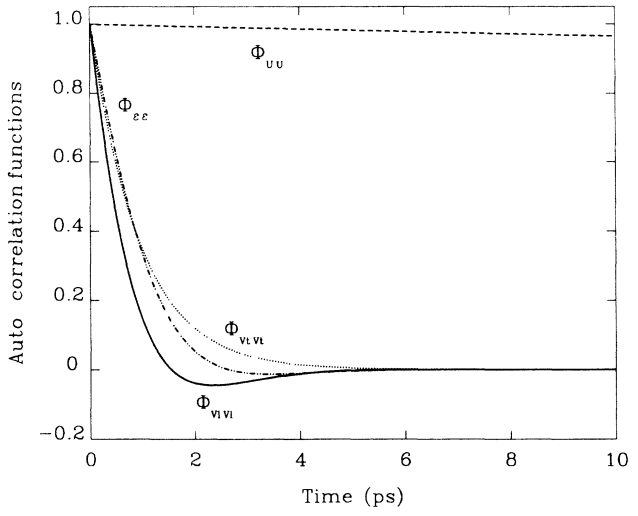

FIG. 9. Autocorrelation functions normalized to their initial values in p-type Si at 77 K with $N_A = 3\times10^{15}$ cm^{-3} at an electric field of 2500 V/cm as a function of time obtained from the expansion into eigenvectors of the matrix α. Continuous, dotted, dashed, and dash-dotted lines refer, respectively, to $\Phi_{v_l v_l}(t)$, $\Phi_{v_t v_t}(t)$, $\Phi_{uu}(t)$, and $\Phi_{\varepsilon\varepsilon}(t)$.

Motivated by these results, we can now use the analytical formulas to obtain information on the physics involved in the problem. The advantage of this procedure is the fact that there the information is strongly compressed: Instead of 11 functions of time we now have only the eigenvalues of the matrix α and for each correlation function $\Phi_{ij}(t)$ at most three expansion coefficients $d_{ij}^{(\nu)}$. Let us first focus on the eigenvalues. They are shown as functions of the electric field in Fig. 11. At low electric fields we have three different real eigenvalues; their inverse can be interpreted as velocity relaxation time, energy relaxation time, and lifetime. Due to the cubic symmetry, at vanishing electric field the velocity relaxaton time is threefold degenerate. With increasing electric field the smallest eigenvalue corresponding to particle number (dash-dotted line) exhibits a slight decrease reflecting the increase of the lifetime with the field. Because recombination processes occur practically only from the bottom of the band, their probability is reduced with increasing carrier energy. Therefore the fraction of free carriers becomes nearly unity and the smallest eigenvalue is only determined by the generation rate. Above a

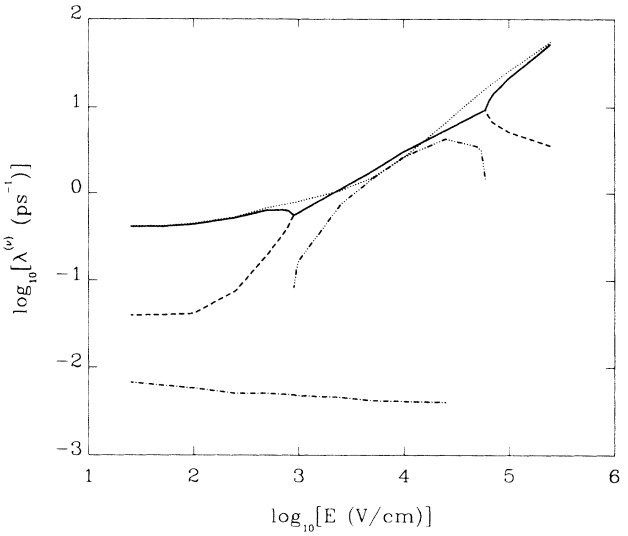

FIG. 11. Eigenvalues of the matrix α as function of the electric field. The solid, dotted, dashed, and dash-dotted lines refer to the eigenvalues corresponding to longitudinal velocity, transverse velocity, energy, and particle number, respectively. In the range between the two critical fields of about 900 and 60 000 V/cm, due to the large coupling between longitudinal velocity and energy, their corresponding eigenvalues are complex conjugate. There, the solid line refers to the real part and the triple-dot dashed line to the imaginary part.

field of about 25 000 V/cm the recombination rate become so small while at the same time the scattering rate becomes so large, that within the MC simulation it is no longer possible to obtain a correlation function for u within a reasonable CPU time. But since at these high fields the coupling between the other variables and u is negligible, it is sufficient to study the system without GR processes.

The other two eigenvalues increase with the field because of the increasing scattering efficiency at higher energies. The energy relaxation rate (dashed line), however, increases much faster than the longitudinal-velocity relaxation rate (solid line) due to the onset of optical phonon emission. At some electric field $E_{\text{crit1}} \approx 900$ V/cm these two eigenvalues become equal and, increasing the field strength further, we have now a pair of complex-conjugate eigenvalues. The solid line in Fig. 9 now corresponds to the real part and the triple-dot dashed line to the imaginary part. In this region velocity and energy relaxation are strongly coupled: Their autocorrelation functions both have the form of Eq. (30) with the same relaxation rate and frequency, only their phases χ are different. The phase of the autocorrelation function of v_l turns out to be always positive, while that of the autocorrelation function of ε is always negative. Thus, as expected, the initial decay of the former one is always faster than that of the latter one. A complex eigenvalue always indicates some kind of ordering in the system. In our case it is the joint action of the electric field and the emission of optical phonons. In its extreme case this is well known as the condition of "streaming motion":[7,8] The carrier is accelerated by the field up to the energy of the optical phonon. From there, by emitting an optical phonon, it is scattered back to the bottom of the band and the cycle starts again. This perfectly periodic limit requires the absence of other scattering mechanisms and an infinite strong phonon emission probability at the threshold energy. In our cases, however, we are far from this limit. The other scattering mechanisms are still efficient and the phonon emission rate is of the order of 10^{12} s^{-1} (cf. Fig. 1 in Ref. 13). Therefore the imaginary part is always smaller than the real part and we never observe more than one oscillation in the correlation functions. When the electric field is increased further, there exists a second critical field $E_{\text{crit2}} \approx 60\,000$ V/cm above which the eigenvalues again become real. At these very high fields, the dissipation in the system is now so strong that no ordering can be maintained anymore.

Another interesting result is that the relaxation rate of the transverse velocity (dotted line) and the real part of the eigenvalue corresponding to the longitudinal velocity (solid line) are in very good agreement over the whole range of the electric field. This means that these quantities still define a relevant time scale also for the longitudinal motion of the carrier system. Thus the fact that the autocorrelation function for v_l decays faster than that for v_t, as can be seen for example in Fig. 5, is a consequence of the coupling between the different variables. As a matter of fact, in the case of complex eigenvalues the large difference in the decay of the correlation functions for ε and v_l is only due to the different values of the phase χ [see Eq. (30)] since both functions are governed by the same pair of eigenvalues. Close to the critical fields E_{crit1} and E_{crit2} there are differences between the transverse and the longitudinal eigenvalues. The former ones are smooth functions of the electric field because they are not affected by the ordering of the system, while the matrix α becomes singular at these fields. This results in a divergence of the eigenvectors if the eigenvalues become equal and the eigenvalues are not analytical functions of the electric field.

Let us now turn to the expansion coefficients $d_{ij}^{(\nu)}$ of the correlation function $\Phi_{ij}(t)$ which give a quantitative measure of the coupling between the different characteristic time scales. The correlation function of the transverse velocities is not considered in the following because they do not couple and are always determined by a single eigenvalue and a single coefficient d. In Figs. 12(a)–12(c) the normalized coefficients $\gamma_{ii}^{(\nu)} = |d_{ii}^{(\nu)}| / \sum_{\mu=1}^{3} |d_{ii}^{(\mu)}|$ are shown as functions of the electric field for each of the three autocorrelation functions, respectively. The solid line corresponds to the largest eigenvalue, the dashed line to the second, and the dash-dotted line to the smallest one. For reasons of simplicity we will refer to them as velocity contribution, energy contribution, and particle number contribution, respectively, as long as they are real, even if this classification is strictly valid only in the absence of coupling. Between the critical fields the coefficients corresponding to the complex-conjugate eigenvalues are also complex conjugate. Thus their absolute values are equal. In this region, additionally we show the absolute value of the ratio between the imagi-

nary and real part of the expansion coefficients (triple-dot dashed line). This ratio determines the phase of the oscillatory contribution [Eq. (30)].

The autocorrelation function of u [Fig. 12(a)] is mainly governed by the lifetime. However, at equilibrium and at small electric fields we find a contribution of the energy relaxation up to nearly 10%. This is because GR processes occur practically only at the bottom of the band. Therefore recombination is strongly affected by the redistribution of the energy due to scattering processes. At increasing electric field, due to the suppression of the recombination, the fraction of free carriers increases and the decay of the autocorrelation function is mainly determined by the generation process and therefore the coupling decreases. Without the electric field, for symmetry reasons the coupling to v_l is zero. It increases up to the first critical field, but never reaches a contribution of more than about 10^{-4}. Thus it is always negligible. Due to the small absolute values of the expansion coefficients above the first critical field, the numerical uncertainty for the ratio between real and imaginary parts is quite large. This may be the reason for its rather irregular shape which, however, for the expansion of the correlation function is irrelevant.

Due to the symmetry of the crystal, at equilibrium the autocorrelation function of v_l [see Fig. 12(b)] cannot couple to the other functions. With increasing fields both other contributions increase. The coupling to u reaches a maximum at a field of about 100 V/cm, but remains always below 10^{-4}. The coupling to ε increases up to the field E_{crit1}, where its coefficient reaches a value of 0.5. As long as the eigenvalues are complex, this value is always

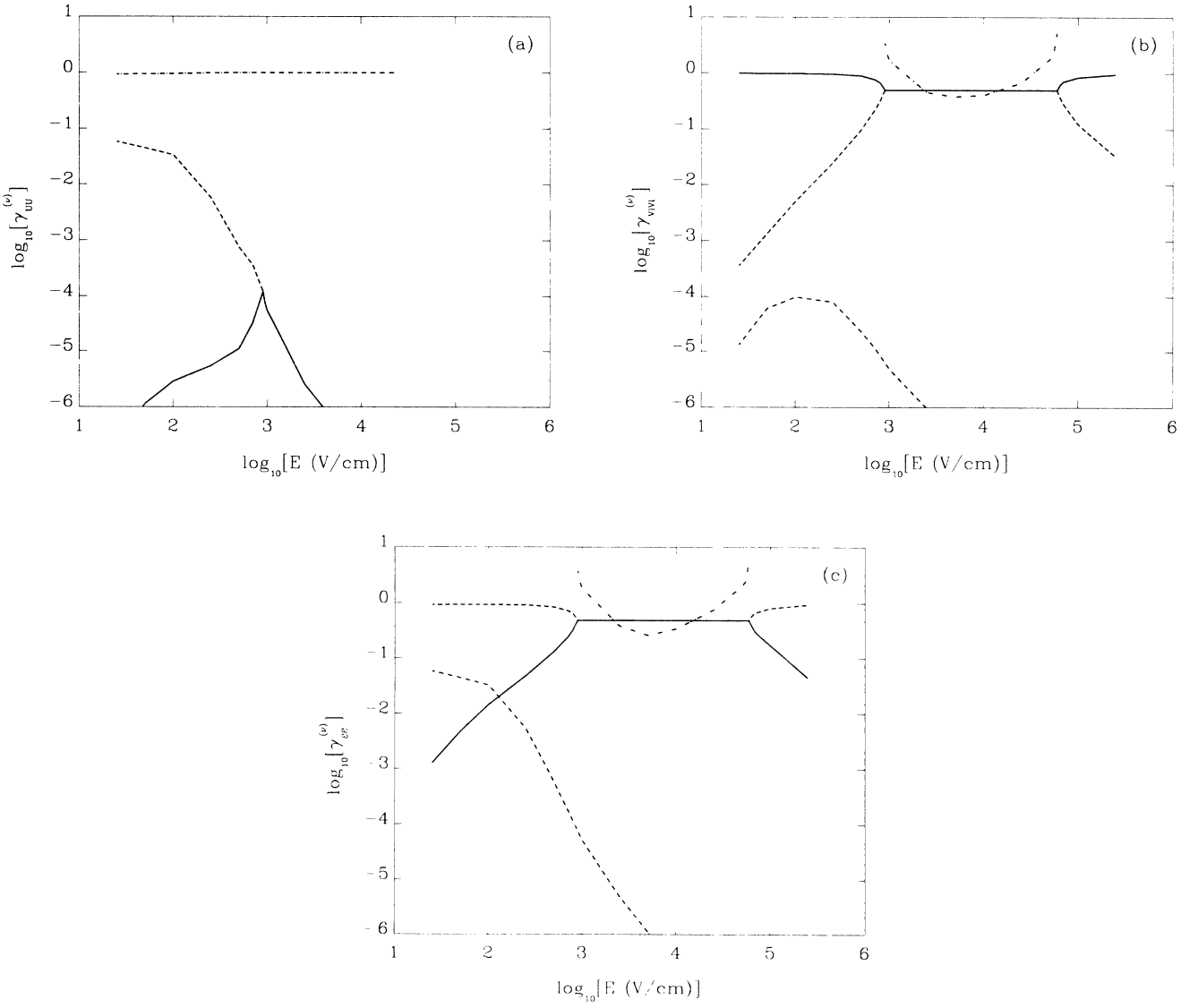

FIG. 12. Expansion coefficients $\gamma_{ii}^{(\nu)}$ of the autocorrelation functions of (a), u, (b) v_l, and (c) ε. Solid, dashed, and dash-dotted lines refer to the corresponding eigenvalues of Fig. 9. In the region of complex-conjugate eigenvalues the triple-dot dashed lines refer to the absolute value of the ratio between the imaginary and real parts of the corresponding expansion coefficient.

the same in order to give a real correlation function. As already mentioned, the ratio between imaginary and real parts is always positive, leading to an initial decay faster than that determined by the real part of the eigenvalue. Above the field E_{crit2}, the coupling coefficients again become different. The contribution of the energy relaxation decreases with increasing difference between the two eigenvalues.

The autocorrelation function of ε [Fig. 12(c)] exhibits the coupling features of both other autocorrelation functions. At low electric fields there is a contribution of about 10% from particle number which decreases with increasing electric field. The coupling to the velocity, on the other hand, is vanishing at low fields, but it increases with increasing field and we obtain the same behavior as for the correlation function of v_l, only the roles of v_l and ε are inverted. The phase in the region of complex eigenvalues now is negative, leading to an initial decay slower than that determined by the real part of the eigenvalue.

For the cross-correlation functions we can plot the same kind of figures for the expansion coefficients but for reasons of brevity they are not shown here. In general, a correlation function between two variables has coefficients corresponding to these two variables at the same order of magnitude. If one of these variables is strongly coupled to the third one, however, all three coefficients are of the same order of magnitude. In the following we will discuss the general features of the cross-correlation functions as shown in Figs. 8 and 10.

The correlation function between v_l and ε follows a well-known behavior.[7] In brief, its structure is related to the energy dependence of the scattering mechanisms, which in the present case always leads to an increase of the scattering rate with increasing energy. Therefore, when considering the correlation function between v_l and ε, we argue as follows: In the positive time region, if initially a positive fluctuation of v_l occurs, at a later time, due to the large absorbed power, a positive fluctuation of ε is likely to occur; for the same reason an initial negative fluctuation of v_l will lead to a negative fluctuation of ε. Thus the initial slope of the correlation function between v_l and ε will always be positive. On the other hand, in the negative time region, we find that if initially a positive fluctuation of ε occurs, at a later time, due to the increased efficiency of the scattering, a negative fluctuation of v_l is likely to occur; for the same reason an initial negative fluctuation of ε will lead to a positive fluctuation of v_l. Thus the initial slope of the correlation function between ε and v_l will always be negative. At short times its behavior is governed by the relaxation time of the longitudinal velocity, while the asymptotic decrease is governed by the energy relaxation time. This function vanishes linearly at lowering field strengths.

As already mentioned, in Eq. (23) the cross-correlation functions between the fraction of free carriers and energy or velocity vanish at zero time because in the case of noninteracting particles these fluctuations are independent. Due to the energy dependence of the recombination and generation probability, however, fluctuations at different times are correlated. An initial positive fluctuation of u leads to an increase in recombination probability near the bottom of the band, thus increasing the average energy of the carriers in the band. Also, an initial negative fluctuation of u leads to a large generation probability at low energies reducing the average energy of the carriers. Therefore the correlation between u and ε increases on the time scale of the energy relaxation time and then returns to zero on the time scale of the lifetime. In the negative time region the function exhibits qualitatively the same structure, since an initial positive (negative) fluctuation in energy leads to a decrease (increase) in recombination probability. Thus it is likely to have a positive (negative) fluctuation in u at later times.

The correlation function between v_l and u has the most complicated structure. In the positive time region its behavior is qualitatively like that of the correlation function between ε and u. Because the recombination and generation processes are symmetric in $\mathbf{k}$ space, the time dependence is mainly governed by the energy fluctuation which is always associated with an initial velocity fluctuation. In the negative time region, however, all three characteristic times scales are important. The reason for this is the following: As already discussed above, a positive fluctuation in u leads to an increase in recombination from the bottom of the band. Since particles with a small velocity are removed, the average velocity increases. But now also the average energy of the carriers increases, leading to a stronger scattering efficiency (see the discussion for the correlation function between v_l and ε). Therefore the velocity decreases below its mean value and the correlation function becomes negative. Finally, on the time scale of the lifetime, the system returns to its stationary state and the correlations disappear. The same arguments hold for the time evolution after an initial negative fluctuation in u.

From the above analysis we conclude the following.

(i) In general, the definition of a relaxation rate for a relevant variable is a complicated task because of the mutual correlations at a microscopic level among the different scattering mechanisms and among the variables themselves. One of the necessary conditions to allow the definition of a relaxation rate, in the sense of an exponential decay of the corresponding correlation function, is that the microscopic times describing the transition processes are decoupled at any value of the carrier energy.

(ii) At equilibrium u and ε are in general coupled while u and $\mathbf{v}$ as well as ε and $\mathbf{v}$ are not. Furthermore, the longitudinal and transverse velocity autocorrelation functions coincide.

(iii) Under linear response in the electric field, u, v_l, and ε are all coupled, but still the longitudinal and transverse velocity autocorrelation functions practically coincide.

(iv) Under nonlinear response even the longitudinal and transverse velocity autocorrelation functions differ.

(v) A rigorous exponential relaxation is expected only at equilibrium for all velocity autocorrelation functions, and, under linear response, for the transverse velocity correlation function.

(vi) Under nonlinear response, a complex relaxation rate can be introduced. Its real part is associated with a thermodynamic character and its imaginary part with a

deterministic character of the carrier ensemble, this latter being responsible for an oscillatory behavior of the correlation functions.

(vii) The MC simulation, by providing an exact solution of the kinetic equation, gives correlation functions which are physically plausible. The analytical approach helps the interpretation, however in general it does not reproduce quantitatively the correct shape of these functions.

V. COMPARISON WITH EXPERIMENTS

The previous sections have shown that the structure of the correlation functions provide much information on the physics of the system. In particular, the analysis of these structures enables one to identify the typical time scales for the relevant variables, but it also demonstrates the limits of the concept of a relaxation time if coupling between different variables becomes important. In general, however, the correlation functions are not directly measurable quantities. Therefore we present in this section the implications of our results for the current spectral density, which is the primary observed quantity in noise measurements.

The current spectral density $S_I(f)$ is defined as twice the Fourier transform of the autocorrelation function of current fluctuations,[16] i.e.,

$$S_I(f)=2\int_{-\infty}^{\infty}\exp(i2\pi ft)\overline{\delta I(0)\delta I(t)}dt \ . \tag{32}$$

[We recall the tensorial character of $S_I(f)$, which in the present case reduces to the longitudinal and transverse component with respect to the applied electric field.] Using the two equivalent forms of the current definition of Eq. (9), also two equivalent expressions for S_I are possible, either in terms of fluctuations of the reduced average velocity, or in terms of the fluctuations of the average velocity and the carrier number (see Ref. 13). The former is useful for a calculation of the spectral density from the MC simulation, since the autocorrelation function of reduced velocity fluctuations is a direct output of the calculations. The latter is better suited for a physical interpretation of the results, since it separates different processes contributing to the total noise.

Figures 13(a)–13(d) report current spectral densities as a function of frequency at different values of the electric field. These are obtained by Fourier transforming the reduced correlation functions directly obtained from the MC simulation. Due to the large difference in the time scales involved in the problem, for each electric field two separate simulations have been performed, one for the short-time and one for the long-time behavior of the correlation functions. This leads to some noise in the results at frequencies corresponding to the transition between the two time scales, which increases with increasing difference between these time scales. The spectral densities are plotted without smoothing procedure in order to provide the reader with an immediate check of the sensitivity of the method.

The results from the MC simulation for the longitudinal current spectral densities are plotted as solid lines, those for the transverse spectral densities as dash-dotted lines. To a very good approximation, in all cases the transverse components exhibit the well-known Lorentzian shape with a cutoff frequency determined by the relaxation rate of the transverse velocity. Therefore we also find a practically perfect agreement between the MC results and the analytical model. In the curves for the longitudinal component, on the other hand, we can clearly identify the different time scales involved. The dashed lines are the spectral densities obtained from the analytical equation for the correlation function [Eq. (27)] using the corresponding eigenvalues and expansion coefficients. We remark that we have not performed a fit of the spectral densities; all parameters are determined by the initial values of the correlation functions and their time derivatives.

At low fields [Fig. 13(a)] the shape of the longitudinal current spectral density corresponds to the sum of two Lorentzians with cutoff frequencies determined by the lifetime and the longitudinal velocity relaxation time. The analytical curve has a too small first plateau and a too large first cutoff frequency. This is due to the microscopic coupling between particle number and energy relaxations which, as discussed above, leads to the nonexponential decay of the particle number autocorrelation function. If in the analytical calculation we use the long-time decay rate of this correlation function (dotted line), we get a perfect agreement with the MC result.

At an intermediate electric field of 2500 V/cm [Fig. 13(b)] the longitudinal spectral densities from the MC simulation and from the analytical model coincide within the numerical uncertainty and are in good agreement with available experimental results.[11,12] At this field we observe the different relaxation times of the longitudinal and transverse velocity. At the end of the second plateau the spectral density shows a slight increase due to the coupling between energy and momentum relaxation. All these features become more evident at the higher electric field of 25 000 V/cm [Fig. 13(c)] where we do not have anymore a second plateau. When the frequency exceeds the value of the inverse lifetime the spectral density decays as a Lorentzian, then reaches a minimum, increases again and, at frequencies large compared to the real and the imaginary part of the corresponding eigenvalue, decreases again with a Lorentzian shape. Except for a slight deviation in the low-frequency value even in this case the agreement between MC and analytical calculation is very good, indicating that a model correlation function with one real and a pair of complex-conjugate rates indeed can be used to analyze current spectral densities.

As already mentioned above, at the highest electric field of 250 000 V/cm the MC simulation has been performed without GR processes. However since we know that these processes do not couple to the other variables, we can estimate their contribution. Therefore, in the analytical results we have added a Lorentzian with a plateau value of $\overline{v}_l^2\overline{u}(1-\overline{u})\tau_l$, where the lifetime τ_l is given by the generation time, and a cutoff frequency of $(2\pi\tau_l)^{-1}$. Figure 13(d) shows the spectral densities for this case using a value $\overline{u}=0.96$ obtained from the extrapolation of the values at lower fields. Even at this large

value of $\bar{u}$ there is still a strong contribution from generation-recombination noise because of the large drift velocity. While at the intermediate fields, due to the large coupling between v_l and ε the high-frequency decay of the longitudinal and the transverse components is quite different, now there is nearly no difference. However, the maximum in the longitudinal spectral density in the frequency range between the relaxation rates of energy and longitudinal velocity is still present.

VI. CONCLUSIONS

In this paper we have presented a detailed analysis of the correlation functions in a doped semiconductor under the influence of an electric field of arbitrary strength. As relevant variables we have considered the number, velocity, and average kinetic energy of the carriers. From the Monte Carlo simulation we have found complicated nonexponential shapes of the autocorrelation functions

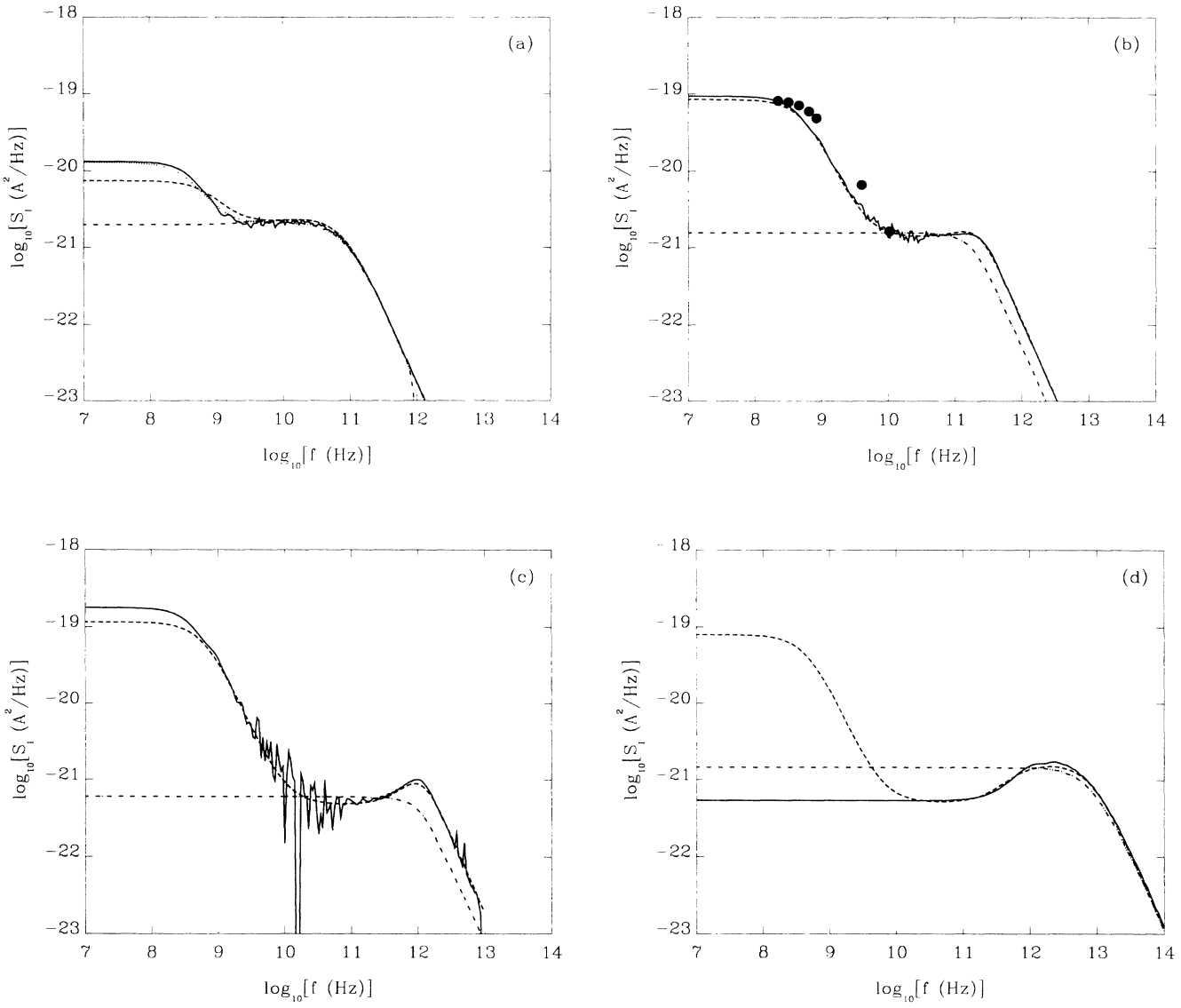

FIG. 13. Current spectral densities as a function of frequency for different values of the electric field. (a) $E=250$ V/cm, (b) $E=2500$ V/cm, (c) $E=25\,000$ V/cm, (d) $E=250\,000$ V/cm. The parameters are $T=77$ K, $N_A=3\times10^{15}$ cm^{-3}, $L=1.5\times10^{-2}$ cm, and $A=3.6\times10^{-3}$ cm^2. The solid and dot-dashed lines refer to the MC simulations for the longitudinal and transverse spectral densities and the dashed lines to the analytical results using the expansion into eigenvectors of the matrix α for the longitudinal case. For the transverse case we obtain a perfect agreement between MC and analytical results for all electric fields. The dotted line in Fig. 13(a) refers to the analytical results for the longitudinal case when the eigenvalues corresponding to u and ε are replaced by the values appropriate to describe the long-time decay. The circles in Fig. 13(b) refer to experimental results (Refs. 9 and 10).

due to the mutual interaction of the relaxation processes of the different variables. The cross-correlation functions exhibit still more complicated structures since, in general, they are influenced by all time scales of the system. In order to get a better physical insight into the problem we have used an analytical model, based on coupled Langevin equations for the relevant variables, leading to coupled first-order differential equations for the correlation functions. The matrix with the coefficients of these equations has been determined from the results of the Monte Carlo calculation. By studying the eigenvalues and eigenvectors of this matrix we then have studied the coupling between different variables.

We have demonstrated for the first time that even at equilibrium the coupling between energy relaxation and generation-recombination processes can lead to a nonexponential decay of the corresponding autocorrelation functions. While this coupling decreases with increasing electric field strength, because hot-carrier conditions reduce the importance of low-energy processes, the coupling between energy and velocity is found to become more important. Above a critical field of about 900 V/cm the character of the eigenvalues changes from three real values to one real and a pair of complex-conjugate values. This indicates the onset of some ordering in the carrier system driven by the electric field. Indeed, this can be identified as the streaming motion, characteristic of the strong interaction with nonpolar optical phonons. Above a second critical field of about 60 000 V/cm the eigenvalues again become real. The dissipation is now so strong that no more ordering is possible.

Using these correlation functions we have calculated the longitudinal and transverse current spectral densities. While the transverse spectral density has always to a very good approximation a Lorentzian shape, the coupling between the different variables leads to a characteristic non-Lorentzian behavior in far from equilibrium conditions. From a comparison with available experiments we conclude that the theory so constructed provides a rigorous basis for the interpretation of noise-spectroscopy measurements in a wide range of frequencies.

ACKNOWLEDGMENTS

This work has been partially supported by the Commission of European Communities (CEC) European Strategic Programme of Research and Development in Information Technology (ESPRIT) II BRA-3017 Project and the Centro di Calcolo of the Modena University. One of us (T.K.) acknowledges support from the Deutsche Forschungsgemeinschaft. The authors wish to thank Dr. P. Bordone, Dr. R. Brunetti, and Dr. C. Jacoboni of the Modena University (Italy), Dr. P. Lugli of the University of Rome II (Italy), Dr. V. Mitin of the Ukranian Academy of Sciences (U.S.S.R.), Dr. C. M. Van Vliet of the University of Montreal (Canada), and Dr. J. P. Nougier and Dr. J. C. Vaissiere of the Montpellier University (France) for valuable discussions concerning the present subject.

APPENDIX A

For the derivation of the relations between the correlation functions and the corresponding reduced quantities, we first notice that there is only one definition of $u(t)$. To simplify the notation we define $u^r(t)=u(t)$. As a consequence, we have

$$\Phi_{uu}=\Phi^r_{uu} \ . \tag{A1}$$

The other four variables are related to the reduced variables according to

$$A(t)=\frac{A^r(t)}{u^r(t)} \ , \tag{A2}$$

where $A=(v_l,v_{t1},v_{t2},\varepsilon)$. Using $\delta A=A(t)-\overline{A}$ and linearizing Eq. (A2) with respect to the fluctuations gives

$$\delta A(t)=\frac{\delta A^r(t)}{\bar{u}}-\frac{\overline{A^r}\delta u^r(t)}{\bar{u}^2}=\frac{1}{\bar{u}}[\delta A^r(r)-\overline{A}\,\delta u(t)] \ . \tag{A3}$$

Thus, for the correlation functions we obtain:

$$\overline{\delta u(0)\delta A(t)}=\frac{1}{\bar{u}}[\overline{\delta u^r(0)\delta A^r(t)}-\overline{A}\,\overline{\delta u^r(0)\delta u^r(t)}] \ , \tag{A4}$$

$$\overline{\delta A(0)\delta u(t)}=\frac{1}{\bar{u}}[\overline{\delta A(0)^r\delta u^r(t)}-\overline{A}\,\overline{\delta u^r(0)\delta u^r(t)}] \ , \tag{A5}$$

$$\begin{aligned}\overline{\delta A(0)\delta B(t)}=\frac{1}{\bar{u}^2}[&\overline{\delta A^r(0)\delta B^r(t)}+\overline{A}\,\overline{B}\,\overline{\delta u^r(0)\delta u^r(t)}\\&-\overline{A}\,\overline{\delta u^r(0)\delta B^r(t)}\\&-\overline{B}\,\overline{\delta A^r(0)\delta u^r(t)}] \ .\end{aligned} \tag{A6}$$

Noticing the fact that for symmetry reasons $\overline{v_{t1}}=\overline{v_{t2}}=0$ Eqs. (A4)–(A6) originate Eqs. (12)–(20).

APPENDIX B

Here we shall prove Eq. (21). Assuming ergodicity, by definition it is

$$\begin{aligned}\overline{\delta A^r(0)\delta B^r(t)}&=\langle\delta A^r(0)\delta B^r(t)\rangle\\&=\frac{1}{N_I^2}\sum_{i,j=1}^{N_I}\langle[A_i^r(0)-\langle A^r\rangle][B_j^r(t)-\langle B^r\rangle]\rangle\\&=\frac{1}{N_I}\langle[A_i^r(0)-\langle A^r\rangle][B_i^r(t)-\langle B^r\rangle]\rangle+\frac{1}{N_I^2}\sum_{\substack{i\neq j\\j=1}}^{N_I}\langle[A_i^r(0)-\langle A^r\rangle][B_j^r(t)-\langle B^r\rangle]\rangle \ ,\end{aligned} \tag{B1}$$

where brackets mean ensemble average.

The off-diagonal term in the last row of Eq. (B1) describes particle-particle correlation, thus for the case of noninteracting particles can be neglected. By applying the above property with $A,B \equiv u(t),\mathbf{v}(t),\varepsilon(t)$, Eq. (21) is directly obtained.

---

*On leave from Institut für Theoretische Physik, Universität, Stuttgart, Pfaffenwaldring 57, D-7000 Stuttgart 80, Federal Republic of Germany.

[1]P. A. McQuarrie, *Statistical Mechanics* (Harper and Row, New York, 1976).

[2]H. B. Callen and T. A. Welton, Phys. Rev. **83**, 34 (1951).

[3]M. Toda, R. Kubo, and N. Saitô, *Statistical Physics I,* Vol. 30 of *Springer Series in Solid-State Science,* edited by M. Cardona, P. Fulde, and H. J. Queisser (Springer-Verlag, Berlin, 1983).

[4]J. J. Niez and D. K. Ferry, Phys. Rev. B **28**, 889 (1983).

[5]J. J. Niez, K. S. Yi, and D. K. Ferry, Phys. Rev. B **28**, 1988 (1983).

[6]R. Brunetti and C. Jacoboni, Phys. Rev. B **29**, 5739 (1984).

[7]P. Lugli, L. Reggiani and J. J. Niez, Phys. Rev. B **40**, 12 382 (1989).

[8]L. Reggiani, *Hot Electron Transport in Semiconductors,* Vol. 58 of *Topics in Applied Physics* (Springer-Verlag, Berlin, 1985).

[9]S. V. Gantsevitch, V. L. Gurevitch, and P. Katilius, Riv. Nuovo Cimento **2**, 1 (1979).

[10]Recent references can be found in the *Proceedings of the 9th Conference on Noise in Physical Systems,* edited by C. M. Van Vliet (World Scientific, Singapore, 1987) and in *Proceedings of the 10th Conference on Noise in Physical Systems,* edited by A. Ambrozy (Akademiai Kiado, Budapest, 1990).

[11]D. Gasquet, B. Azais, J. C. Vaissiere, and J. P. Nougier, in *Noise in Physical Systems and 1/f Noise—1985,* edited by A. D'Amico and P. Mazzetti (North-Holland, Amsterdam, 1985), p. 231.

[12]J. C. Vaissiere, Ph.D. dissertation, University of Montpellier, 1986 (unpublished).

[13]T. Kuhn, L. Reggiani, L. Varani, and V. Mitin, Phys. Rev. B **42**, 5702 (1990).

[14]C. Jacoboni and L. Reggiani, Rev. Mod. Phys. **55**, 645 (1983).

[15]L. Reggiani, R. Brunetti, and E. Normantas, J. Appl. Phys. **59**, 1212 (1986).

[16]A. van der Ziel, *Noise in Solid State Devices and Circuits* (Wiley and Sons, New York, 1986).